Autonomous Robots 19, 219–232, 2005

Locomotion Control of a Biped Robot Using Nonlinear Oscillators

SHINYA AOI AND KAZUO TSUCHIYA
Dept. of Aeronautics and Astronautics, Graduate School of Engineering, Kyoto University, Yoshida-honmachi, Sakyo-ku, Kyoto, 606-8501, Japan

Abstract. Recently, many experiments and analyses with biped robots have been carried out. Steady walking of a biped robot implies a stable limit cycle in the state space of the robot. In the design of a locomotion control system, there are primarily three problems associated with achieving such a stable limit cycle: the design of the motion of each limb, interlimb coordination, and posture control. In addition to these problems, when environmental conditions change or disturbances are added to the robot, there is the added problem of obtaining robust walking against them. In this paper we attempt to solve these problems and propose a locomotion control system for a biped robot to achieve robust walking by the robot using nonlinear oscillators, each of which has a stable limit cycle. The nominal trajectories of each limb's joints are designed by the phases of the oscillators, and the interlimb coordination is designed by the phase relation between the oscillators. The phases of the oscillators are reset and the nominal trajectories are modified using sensory feedbacks that depend on the posture and motion of the robot to achieve stable and robust walking. We verify the effectiveness of the proposed locomotion control system, analyzing the dynamic properties of the walking motion by numerical simulations and hardware experiments.

Keywords: biped robot, locomotion control, limit cycle, nonlinear oscillators, phase reset, touch sensor signal

1. Introduction

Over the last few years, many experiments and analyses have been carried out on biped robots. Steady walking by a biped robot implies a stable limit cycle in the state space of the robot. In the design of a locomotion control system for a biped robot, there are primarily three problems associated with achieving such a stable limit cycle. The first problem is the difficulty in designing the motion of each limb on the robot, and the second is the interlimb coordination. A biped robot is a mechanical system composed of many links that are connected with others by rotary joints, and in general has poor stability in three-dimensional walking. Therefore, it is difficult to design walking motions and the relation to obtain such a stable limit cycle. To date, many researchers have attempted to achieve trajectories of joints using optimization (Roussel et al., 1998; Chevallereau and Aoustin, 2001; Ono and Liu, 2002; Bessonnet et al., 2004). Also, many experiments and analyses have been conducted (Yamaguchi et al., 1999; Kagami et al., 2002; Kajita et al., 2002; Löffler et al., 2003; Nagasaki et al., 2004) based on the zero moment point (ZMP) criterion (Vukobratović et al., 1990). The third problem is the posture control arising from underactuation (Goswami, 1999). All the joints of the robot have motors that control the joints' motions; however, the robot has no actuator in the foot that directly controls its posture and motion. Thus, it is difficult to stabilize the posture and motion, especially when the robot is supported by only one leg. In addition to these three problems, when environmental situations change or disturbances are added to the robot, there arise further obstacles to achieving robust walking.

In a system that has a stable limit cycle, trajectories near the limit cycle can be approximately described by the phase of a nonlinear oscillator (Kuramoto, 1984). When some such nonlinear oscillators have interactions with each other, which are given only by the phases (phase dynamics), the phase relation between the limit cycles is obtained. In this paper, we attempt to solve the

above problems and also propose a locomotion control system for a biped robot to achieve robust walking of it by employing such nonlinear oscillators and extending the locomotion control system for a quadruped robot developed in our previous work (Tsujita et al., 2001). In the proposed locomotion control system, regarding the first problem, we design nominal trajectories of the joints of each limb by the phase of such a nonlinear oscillator to attain a stable periodic motion of a limb. That is, a nominal motion of the robot's joint controlled by a motor is given by a map from the state of a stable limit cycle. Then, since the motion of each limb is given by the phase of an oscillator, the interlimb coordination is obtained via the phase relation between the oscillators. As for the second problem, the oscillators interact with each other through phase dynamics based on a nominal gait pattern to achieve interlimb coordination. Finally, to the third and additional problems, the phases of the oscillators are reset and the nominal trajectories of the joints are modified using sensory feedbacks that depend on the posture and motion of the robot to realize stable and robust walking.

In this paper, using the proposed locomotion control system, we conduct numerical simulations and hardware experiments to investigate whether a biped robot achieves robust walking despite environmental changes and disturbances, and analyze dynamic properties of the walking motion. This paper is organized as follows: Section 2 introduces the model for a specific biped robot, and Section 3 proposes a locomotion control system for the biped robot. The effectiveness of the proposed locomotion control system is verified by numerical simulations in Section 4, and by hardware experiments in Section 5. Section 6 includes a discussion and conclusion.

2. Model of Biped Robot

Figure 1 shows the biped robot considered in this paper, consisting of a trunk, a pair of arms composed of four links, and a pair of legs composed of six links. Each link is connected to the others through a single degree of freedom rotational joint. A motor is installed at each joint. Left and right legs are numbered Legs 1 and 2, respectively. The joints of the legs are also numbered Joints 1 . . . 6 from the side of the trunk, where Joints 1, 2, and 3 are yaw, roll, and pitch hip joints, respectively, Joint 4 is a pitch knee joint, and Joints 5 and 6 are pitch and roll ankle joints. The arms are also numbered in a similar manner. Four touch sensors are attached to the sole of each foot, enumerated from Sensor 1 to 4 at each leg.

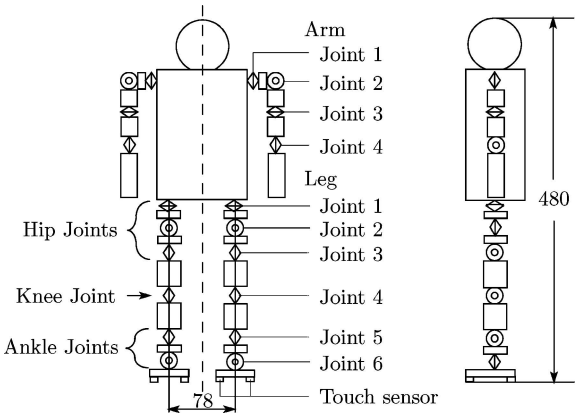

Figure 1. Schematic model of a biped robot [mm]. The robot has a trunk, a pair of arms composed of four links, and a pair of legs composed of six links. Each link is connected to the others through a single degree of freedom rotational joint. Leg joints consist of hip, knee, and ankle joints. The hip joint has yaw, roll, and pitch joints, the knee joint consists of a pitch joint, and the ankle joint is composed of pitch and roll joints. Four touch sensors are attached to the sole of each foot.

Coordinate axes $\{\boldsymbol{a}_0\} = \{\boldsymbol{a}_{01}\ \boldsymbol{a}_{02}\ \boldsymbol{a}_{03}\}$ are fixed to the ground, where axis $\boldsymbol{a}_{01}$ is in the nominal walking direction, axis $\boldsymbol{a}_{02}$ is in the lateral direction, and axis $\boldsymbol{a}_{03}$ is in the vertical direction. Coordinate axes $\{\boldsymbol{a}_{\mathrm{T}}\} = \{\boldsymbol{a}_{\mathrm{T}1}\ \boldsymbol{a}_{\mathrm{T}2}\ \boldsymbol{a}_{\mathrm{T}3}\}$ are fixed in the trunk, where axis $\boldsymbol{a}_{\mathrm{T}1}$ is the front-to-back axis and axis $\boldsymbol{a}_{\mathrm{T}2}$ is the side-to-side axis. The origin of axes $\{\boldsymbol{a}_{\mathrm{T}}\}$ is at the center of mass of the trunk. The position vector of the trunk is given by $r_0^{\mathrm{T}} = [\, r_{01}\ \ r_{02}\ \ r_{03}\,]$ in axes $\{\boldsymbol{a}_0\}$. The posture of the trunk is expressed as Euler angles $\theta_{\mathrm{T}}^{\mathrm{T}} = [\, \theta_{\mathrm{T}1}\ \ \theta_{\mathrm{T}2}\ \ \theta_{\mathrm{T}3}]$ in axes $\{\boldsymbol{a}_{\mathrm{T}}\}$. When these angles are small, angles $\theta_{\mathrm{T}1}$, $\theta_{\mathrm{T}2}$, and $\theta_{\mathrm{T}3}$, called roll, pitch, and yaw angles, are the rotation angles around axes $\boldsymbol{a}_{\mathrm{T}1}$, $\boldsymbol{a}_{\mathrm{T}2}$, and $\boldsymbol{a}_{\mathrm{T}3}$, respectively (see Fig. 2). The rotation angles of Joint j of Arm i and Joint k of Leg i are also expressed as $\theta_{\mathrm{A}j}^{(i)}$ and $\theta_{\mathrm{L}k}^{(i)}$, respectively ($i = 1, 2$, $j = 1, \ldots, 4$, $k = 1, \ldots, 6$).

Here, state variable $q \in \mathbb{R}^{26}$ is introduced by

$$q^{\mathrm{T}} = \left[\, r_{0i} \quad \theta_{\mathrm{T}i} \quad \theta_{\mathrm{A}j}^{(1)} \quad \theta_{\mathrm{A}j}^{(2)} \quad \theta_{\mathrm{L}k}^{(1)} \quad \theta_{\mathrm{L}k}^{(2)} \,\right] \qquad i = 1, 2, 3,\ \ j = 1, \ldots, 4,\ \ k = 1, \ldots, 6 \tag{1}$$

Equations of motion for state variable q are derived using Lagrangian equations and are written by

$$M(q)\ddot{q} + H(q, \dot{q}) = G + U + \Lambda \tag{2}$$

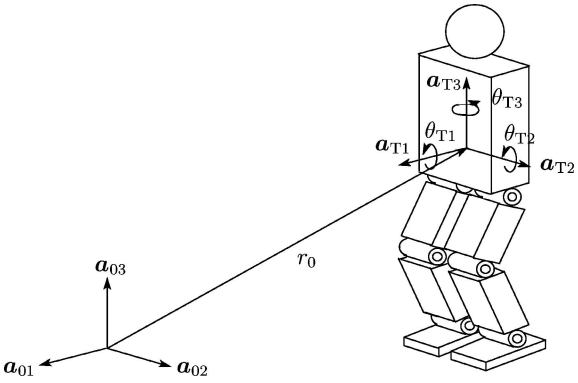

Figure 2. Coordinate axes $\{\boldsymbol{a}_0\} = \{\boldsymbol{a}_{01}\ \boldsymbol{a}_{02}\ \boldsymbol{a}_{03}\}$ fixed to the ground and $\{\boldsymbol{a}_T\} = \{\boldsymbol{a}_{T1}\ \boldsymbol{a}_{T2}\ \boldsymbol{a}_{T3}\}$ fixed in the trunk, position vector r_0 of the trunk, and Euler angles θ_{T1}, θ_{T2}, and θ_{T3}.

where $M(q) \in \mathbb{R}^{26\times 26}$ is the generalized mass matrix, $H(q, \dot{q}) \in \mathbb{R}^{26}$ is the nonlinear term that includes Coriolis and centrifugal forces, $G \in \mathbb{R}^{26}$ is the gravity term, $U \in \mathbb{R}^{26}$ is the input torque term, and $\Lambda \in \mathbb{R}^{26}$ is the reaction force term from the ground. The ground is modeled as a spring with a damper (see Appendix A). In this paper, numerical simulations are carried out based on the equations of motion.

3. Locomotion Control

3.1. *Locomotion Control System*

The locomotion control system consists of a motion generator and a motion controller (see Fig. 3). The motion generator comprises a rhythm generator and a trajectory generator. The rhythm generator has two types of oscillators: Motion Oscillators and Inter Oscillator (see Fig. 4). As Motion Oscillators, there are Leg 1, Leg 2, Arm 1, Arm 2, and Trunk Oscillators. The trajectory generator encodes the nominal trajectories of all the joints by the phases of Motion Oscillators. For example, the trajectory generator encodes the nominal trajectories of the joints of Leg 1 by the phase of Leg 1 Oscillator. The nominal trajectories are sent to the motion controller, in which motor controllers manipulate the motions of the joints using the nominal trajectories as command signals. Inter Oscillator interacts with Motion Oscillators. Specifically, Inter Oscillator affects Arm 1, Arm 2, and Trunk Oscillators and interacts with Leg 1 and Leg 2 Oscillators. These interactions determine the interlimb coordination, that is, the phase differences between the oscillators, thus forming

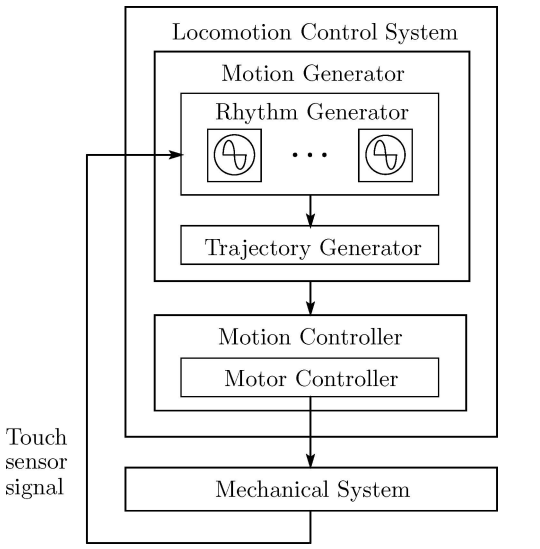

Figure 3. Locomotion control system. The locomotion control system consists of a motion controller and a motion generator. The motion controller is composed of motor controllers that manipulate the motions of the joints. The motion generator has a rhythm generator and a trajectory generator. In the rhythm generator, there are two types of oscillators, Motion Oscillators and Inter Oscillator. The trajectory generator encodes all the nominal trajectories of the joints by the phases of Motion Oscillators, which are sent to the motion controller. At the foot's landing on the ground, a feedback signal is returned to the locomotion control system from the touch sensor of the leg.

a gait pattern for the biped robot. When the foot of Leg i lands on the ground, a sensory signal is fed back to the locomotion control system from the touch sensor, and Leg i Oscillator receives the touch sensor signal ($i = 1, 2$).

3.2. *Design of Nominal Joint Trajectories*

Here, the nominal trajectories of all the joints are designed by the phases of Motion Oscillators in the following way: First, the nominal trajectories of the feet, specifically Joint 5 of the legs, are expressed in coordinate axes $\{\boldsymbol{a}_T\}$ fixed in the trunk, and are encoded by the phases of Leg Oscillators. Similarly to the nominal foot trajectories, the nominal trajectories of the hands are also expressed in axes $\{\boldsymbol{a}_T\}$ and are encoded by the phases of Arm Oscillators. The nominal trajectories of the joints are then calculated based on the inverse kinematics. Next, since the nominal trajectories of the joints of each limb are designed by the phase of the corresponding oscillator, the interlimb coordination is obtained by the phase differences between

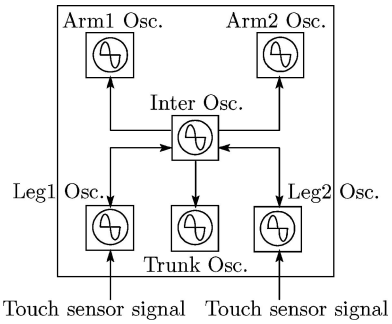

Figure 4. Rhythm generator. The rhythm generator consists of Leg 1, Leg 2, Arm 1, Arm 2, Trunk, and Inter Oscillators. Inter Oscillator has interactions with the other oscillators. Specifically, Inter Oscillator affects Arm 1, Arm 2, and Trunk Oscillators and interacts with Leg 1 and Leg 2 Oscillators. When the foot of Leg i touches the ground, Leg i Oscillator receives a touch sensor signal ($i = 1, 2$).

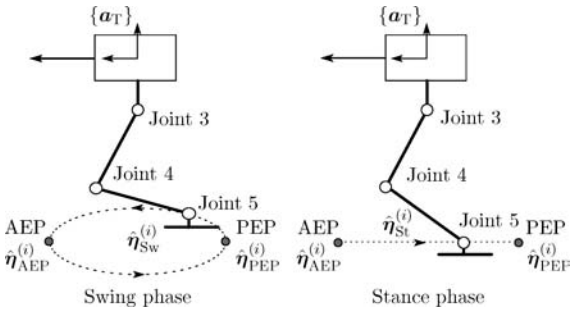

Figure 5. Nominal foot trajectory. The nominal foot trajectory of Leg i consists of nominal foot trajectory $\hat{\eta}^{(i)}_{Sw}$ for the swing phase that is designed as a simple closed curve and nominal foot trajectory $\hat{\eta}^{(i)}_{St}$ for the stance phase that is given as a straight line ($i = 1, 2$). The nominal swing phase changes into the nominal stance phase at AEP and the nominal stance phase shifts to the nominal swing phase at PEP. These trajectories are expressed in axes $\{\boldsymbol{a}_T\}$ fixed in the trunk.

the oscillators. Therefore, from a nominal gait pattern, the nominal phase differences between the oscillators are designed that give the interactions between the oscillators. Finally, the posture and motion of the trunk required for the robot to walk stably is designed by an analysis based on the inverse dynamics and numerical simulations.

In the following, we explain the design procedure in more detail. First, the phases of Leg i, Arm i, Trunk, and Inter Oscillators are introduced, expressed by $\phi^{(i)}_L$, $\phi^{(i)}_A$, ϕ_T, and ϕ_I, respectively ($i = 1, 2$). Then, the nominal trajectory of the foot, specifically Joint 5 of the leg, is designed (see Fig. 5). To do this, two nominal positions of the foot are introduced into coordinate axes $\{\boldsymbol{a}_T\}$ fixed in the trunk: the anterior extreme position (AEP) and the posterior extreme position (PEP) of Leg i expressed as $\hat{\eta}^{(i)T}_{AEP} = [\,\hat{\eta}^{(i)}_{AEP1}\ \hat{\eta}^{(i)}_{AEP2}\ \hat{\eta}^{(i)}_{AEP3}\,]$ and $\hat{\eta}^{(i)T}_{PEP} = [\,\hat{\eta}^{(i)}_{PEP1}\ \hat{\eta}^{(i)}_{PEP2}\ \hat{\eta}^{(i)}_{PEP3}\,]$, respectively ($i = 1, 2$). From now on, $\hat{*}$ indicates the nominal value of $*$. In axes $\{\boldsymbol{a}_T\}$, the nominal foot trajectory of Leg i for the swing phase is designed as a simple closed curve $\hat{\eta}^{(i)T}_{Sw} = [\,\hat{\eta}^{(i)}_{Sw1}\ \hat{\eta}^{(i)}_{Sw2}\ \hat{\eta}^{(i)}_{Sw3}\,]$ that involves points $\hat{\eta}^{(i)}_{AEP}$ and $\hat{\eta}^{(i)}_{PEP}$ ($i = 1, 2$), and the nominal foot trajectory of Leg i for the stance phase is given as a straight line $\hat{\eta}^{(i)T}_{St} = [\,\hat{\eta}^{(i)}_{St1}\ \hat{\eta}^{(i)}_{St2}\ \hat{\eta}^{(i)}_{St3}\,]$ that also includes points $\hat{\eta}^{(i)}_{AEP}$ and $\hat{\eta}^{(i)}_{PEP}$ ($i = 1, 2$). Note that since nominal foot trajectory $\hat{\eta}^{(i)}_{St}$ for the stance phase is designed to move in the opposite walking direction in axes $\{\boldsymbol{a}_T\}$ and in fact the foot is constrained on the ground during the stance phase, the foot does not move, and the trunk moves in the walking direction in axes $\{\boldsymbol{a}_0\}$ fixed to the ground. Both in the nominal swing and stance phases, the nominal movement of the foot is designed so as to be parallel to the line that involves points AEP and PEP. The nominal foot trajectory of Leg i is expressed in axes $\{\boldsymbol{a}_T\}$ as $\hat{\eta}^{(i)T}_L = [\,\hat{\eta}^{(i)}_{L1}\ \hat{\eta}^{(i)}_{L2}\ \hat{\eta}^{(i)}_{L3}\,]$ ($i = 1, 2$) and is generated using one of the two nominal trajectories alternatively, that is, the nominal swing phase changes into the nominal stance phase at point AEP and the nominal stance phase shifts to the nominal swing phase at point PEP. Next, nominal foot trajectories $\hat{\eta}^{(i)}_{Sw}$ and $\hat{\eta}^{(i)}_{St}$ are expressed as the functions of phase $\phi^{(i)}_L$ of Leg i Oscillator, where $\hat{\eta}^{(i)}_{Sw} = \hat{\eta}^{(i)}_{Sw}(\phi^{(i)}_L)$ and $\hat{\eta}^{(i)}_{St} = \hat{\eta}^{(i)}_{St}(\phi^{(i)}_L)$, respectively ($i = 1, 2$). The nominal phases of Leg i Oscillator at points AEP and PEP ($i = 1, 2$) are expressed as $\hat{\phi}_{AEP}$ and $\hat{\phi}_{PEP}(= 0, 2\pi)$, respectively. Finally, nominal foot trajectory $\hat{\eta}^{(i)}_L$ of Leg i is expressed as the function of phase $\phi^{(i)}_L$ of Leg i Oscillator ($i = 1, 2$) (see Appendix B) by

$$\hat{\eta}^{(i)}_L\left(\phi^{(i)}_L\right) = \begin{cases} \hat{\eta}^{(i)}_{Sw}\left(\phi^{(i)}_L\right) & 0 \le \phi^{(i)}_L < \hat{\phi}_{AEP} \\ \hat{\eta}^{(i)}_{St}\left(\phi^{(i)}_L\right) & \hat{\phi}_{AEP} \le \phi^{(i)}_L < 2\pi \end{cases} \quad i = 1, 2 \tag{3}$$

The inverse kinematics gives nominal trajectories $\hat{\theta}^{(i)}_{L3}$ of Joint 3 (the pitch hip joint), $\hat{\theta}^{(i)}_{L4}$ of Joint 4 (the pitch knee joint), and $\hat{\theta}^{(i)}_{L5}$ of Joint 5 (the pitch ankle joint) of Leg i by the functions of phase $\phi^{(i)}_L$ of Leg i Oscillator ($i = 1, 2$) as follows:

$$\hat{\theta}^{(i)}_{Lj} = \hat{\theta}^{(i)}_{Lj}\left(\phi^{(i)}_L\right) \quad i = 1, 2,\ j = 3, 4, 5 \tag{4}$$

The nominal trajectories of the hands are designed in a similar way. In particular, the arms are driven so that

the hands oscillate in the pitch plane; nominal trajectory $\hat{\theta}_{\mathrm{A1}}^{(i)}$ of Joint 1 of Arm i is given as the function of phase $\phi_{\mathrm{A}}^{(i)}$ of Arm i Oscillator ($i = 1, 2$) by

$$\hat{\theta}_{\mathrm{A1}}^{(i)} = \hat{\theta}_{\mathrm{A1}}^{(i)}\left(\phi_{\mathrm{A}}^{(i)}\right) = \hat{A}\cos\phi_{\mathrm{A}}^{(i)} \quad i = 1, 2 \tag{5}$$

where $\hat{A}$ is the nominal amplitude of the arm motion. Nominal trajectories $\hat{\theta}_{\mathrm{A2}}^{(i)}$, $\hat{\theta}_{\mathrm{A3}}^{(i)}$, and $\hat{\theta}_{\mathrm{A4}}^{(i)}$ of Joints 2, 3, and 4 of Arm i are fixed so that $\hat{\theta}_{\mathrm{A2}}^{(i)} = 0$, $\hat{\theta}_{\mathrm{A3}}^{(i)} = 0$, and $\hat{\theta}_{\mathrm{A4}}^{(i)} = \pi/2$, respectively ($i = 1, 2$).

Second, the nominal phase differences between the oscillators are designed based on nominal gait patterns. The nominal gait patterns are given so that both arms and both legs move out of phase and one arm and the contralateral leg move in phase. That is, nominal phase $\hat{\phi}_{\mathrm{L}}^{(i)}$ of Leg i Oscillator and nominal phase $\hat{\phi}_{\mathrm{A}}^{(i)}$ of Arm i Oscillator ($i = 1, 2$) are designed by nominal phase $\hat{\phi}_{\mathrm{I}}$ of Inter Oscillator by

$$\begin{cases} \hat{\phi}_{\mathrm{A}}^{(i)} = \hat{\phi}_{\mathrm{I}} - (-1)^i\pi/2 \\ \hat{\phi}_{\mathrm{L}}^{(i)} = \hat{\phi}_{\mathrm{I}} + (-1)^i\pi/2 \end{cases} \quad i = 1, 2 \tag{6}$$

On the other hand, nominal phase $\hat{\phi}_{\mathrm{T}}$ of Trunk Oscillator may be designed arbitrarily; here, it is designed by nominal phase $\hat{\phi}_{\mathrm{I}}$ of Inter Oscillator by

$$\hat{\phi}_{\mathrm{T}} = \hat{\phi}_{\mathrm{I}} \tag{7}$$

The phase dynamics of the oscillators are defined as

$$\begin{cases} \dot{\phi}_{\mathrm{I}} &= \hat{\omega} + g_{1\mathrm{I}} \\ \dot{\phi}_{\mathrm{T}} &= \hat{\omega} + g_{1\mathrm{T}} \\ \dot{\phi}_{\mathrm{A}}^{(i)} &= \hat{\omega} + g_{1\mathrm{A}}^{(i)} \quad i = 1, 2 \\ \dot{\phi}_{\mathrm{L}}^{(i)} &= \hat{\omega} + g_{1\mathrm{L}}^{(i)} \quad i = 1, 2 \end{cases} \tag{8}$$

where $\hat{\omega}$ is the nominal angular velocity of each oscillator and $g_{1\mathrm{I}}$, $g_{1\mathrm{T}}$, $g_{1\mathrm{A}}^{(i)}$, and $g_{1\mathrm{L}}^{(i)}$ ($i = 1, 2$) are the terms derived from the interactions between the oscillators in the following way: First, in order that the nominal gait patterns in Eqs. (6) and (7) are formed, potential functions V_{I}, V_{T}, $V_{\mathrm{A}}^{(i)}$, and $V_{\mathrm{L}}^{(i)}$ ($i = 1, 2$) are derived by

$$\begin{cases} V_{\mathrm{I}} &= -\sum_{i=1}^{2} K_{\mathrm{L}}\cos\left(\phi_{\mathrm{I}} - \phi_{\mathrm{L}}^{(i)} + (-1)^i\pi/2\right) \\ V_{\mathrm{T}} &= -K_{\mathrm{T}}\cos(\phi_{\mathrm{T}} - \phi_{\mathrm{I}}) \\ V_{\mathrm{A}}^{(i)} &= -K_{\mathrm{A}}\cos\left(\phi_{\mathrm{A}}^{(i)} - \phi_{\mathrm{I}} + (-1)^i\pi/2\right) \quad i = 1, 2 \\ V_{\mathrm{L}}^{(i)} &= -K_{\mathrm{L}}\cos\left(\phi_{\mathrm{L}}^{(i)} - \phi_{\mathrm{I}} - (-1)^i\pi/2\right) \quad i = 1, 2 \end{cases} \tag{9}$$

where K_{L}, K_{A}, and K_{T} are gain constants. Functions $g_{1\mathrm{I}}$, $g_{1\mathrm{T}}$, $g_{1\mathrm{A}}^{(i)}$, and $g_{1\mathrm{L}}^{(i)}$ are derived by

$$\begin{aligned} &g_{1\mathrm{I}} = -\frac{\partial V_{\mathrm{I}}}{\partial\phi_{\mathrm{I}}}, \quad g_{1\mathrm{T}} = -\frac{\partial V_{\mathrm{T}}}{\partial\phi_{\mathrm{T}}}, \quad g_{1\mathrm{A}}^{(i)} = -\frac{\partial V_{\mathrm{A}}^{(i)}}{\partial\phi_{\mathrm{A}}^{(i)}}, \\ &g_{1\mathrm{L}}^{(i)} = -\frac{\partial V_{\mathrm{L}}^{(i)}}{\partial\phi_{\mathrm{L}}^{(i)}} \quad i = 1, 2 \end{aligned} \tag{10}$$

As a result, functions $g_{1\mathrm{I}}$, $g_{1\mathrm{T}}$, $g_{1\mathrm{A}}^{(i)}$, and $g_{1\mathrm{L}}^{(i)}$ are written as

$$\begin{cases} g_{1\mathrm{I}} &= -\sum_{i=1}^{2} K_{\mathrm{L}}\sin\left(\phi_{\mathrm{I}} - \phi_{\mathrm{L}}^{(i)} + (-1)^i\pi/2\right) \\ g_{1\mathrm{T}} &= -K_{\mathrm{T}}\sin(\phi_{\mathrm{T}} - \phi_{\mathrm{I}}) \\ g_{1\mathrm{A}}^{(i)} &= -K_{\mathrm{A}}\sin\left(\phi_{\mathrm{A}}^{(i)} - \phi_{\mathrm{I}} + (-1)^i\pi/2\right) \quad i = 1, 2 \\ g_{1\mathrm{L}}^{(i)} &= -K_{\mathrm{L}}\sin\left(\phi_{\mathrm{L}}^{(i)} - \phi_{\mathrm{I}} - (-1)^i\pi/2\right) \quad i = 1, 2 \end{cases} \tag{11}$$

Thirdly, the nominal trajectories of the posture and motion of the trunk are designed. Since the biped robot walks in three-dimensional space, it is liable to fall over laterally, especially when it is supported by only one leg. Therefore, the nominal trajectories of the roll hip and the roll ankle joints are designed so that the roll motion of the trunk achieves a periodic motion whose cycle is similar to the step cycle and compensates for the lateral motion, preventing the robot from falling over laterally. Thus, nominal trajectories $\hat{\theta}_{\mathrm{L2}}^{(i)}$ of Joint 2 (the roll hip joint) and $\hat{\theta}_{\mathrm{L6}}^{(i)}$ of Joint 6 (the roll ankle joint) of Leg i ($i = 1, 2$) are given as the functions of phase ϕ_{T} of Trunk Oscillator by

$$\begin{aligned} \hat{\theta}_{\mathrm{L2}}^{(i)} &= \hat{\theta}_{\mathrm{L2}}^{(i)}(\phi_{\mathrm{T}}) = \hat{B}\cos(\phi_{\mathrm{T}} + \hat{\psi}) - (-1)^i\hat{\delta} \\ \hat{\theta}_{\mathrm{L6}}^{(i)} &= \hat{\theta}_{\mathrm{L6}}^{(i)}(\phi_{\mathrm{T}}) = -\hat{B}\cos(\phi_{\mathrm{T}} + \hat{\psi}) + (-1)^i\hat{\delta} \\ & \qquad\qquad i = 1, 2 \end{aligned} \tag{12}$$

where $\hat{B}$ and $\hat{\psi}$ are the nominal amplitude and the nominal phase of the roll motion, and $\hat{\delta}$ is the nominal bias angle of the roll motion to avoid a collision of the legs. Moreover, nominal trajectory $\hat{\theta}_{\mathrm{L3}}^{(i)}$ of Joint 3 (the pitch hip joint) of Leg i is modified from $\hat{\theta}_{\mathrm{L3}}^{(i)}(\phi_{\mathrm{L}}^{(i)})$ obtained in Eq. (4) to $\hat{\theta}_{\mathrm{L3}}^{(i)}(\phi_{\mathrm{L}}^{(i)}) - \hat{C}$ ($i = 1, 2$) so that the trunk maintains pitch angle $\hat{C}$ in axes $\{\boldsymbol{a}_0\}$ fixed to the ground. To avoid the yaw of the trunk in axes $\{\boldsymbol{a}_0\}$, nominal trajectory $\hat{\theta}_{\mathrm{L1}}^{(i)}$ of Joint 1 (the yaw hip joint) of Leg i ($i = 1, 2$) is designed by

$$\hat{\theta}_{\mathrm{L1}}^{(i)} = 0 \quad i = 1, 2 \tag{13}$$

Finally, we introduce some parameters that characterize the locomotion. The ratio between the nominal stance phase duration and the nominal step cycle is expressed by nominal duty ratio $\hat{\beta}$ $(0 < \beta < 1)$. Then, nominal phase $\hat{\phi}_{\mathrm{AEP}}$ of Leg Oscillators at point AEP is given by

$$\hat{\phi}_{\mathrm{AEP}} = 2\pi(1-\hat{\beta}) \tag{14}$$

Nominal angular velocity $\hat{\omega}$ of each oscillator in Eq. (8) is expressed by

$$\hat{\omega} = 2\pi \frac{1-\hat{\beta}}{\hat{T}_{\mathrm{Sw}}} \tag{15}$$

where $\hat{T}_{\mathrm{Sw}}$ is the nominal swing phase duration. The nominal stride of Leg i is expressed by $\hat{S}^{(i)}$, which indicates the distance between points AEP and PEP of Leg i $(i = 1, 2)$ (see Fig. 5). In particular, $\hat{S}^{(1)} = \hat{S}^{(2)} (\equiv \hat{S})$ is used, and then nominal locomotion speed $\hat{v}$ is obtained by

$$\hat{v} = \frac{1-\hat{\beta}}{\hat{\beta}} \frac{\hat{S}}{\hat{T}_{\mathrm{Sw}}} \tag{16}$$

3.3. Trajectory Control

All the joints are controlled using the local Proportional-Derivative (PD) feedback controller, where the nominal trajectories of the joints are used as command signals. Thus, the input torques at the joints are given by

$$\begin{aligned} u_{\mathrm{A}j}^{(i)} &= -K_{\mathrm{PA}j}^{(i)}\left(\theta_{\mathrm{A}j}^{(i)} - \hat{\theta}_{\mathrm{A}j}^{(i)}\right) - K_{\mathrm{DA}j}^{(i)}\left(\dot{\theta}_{\mathrm{A}j}^{(i)} - \dot{\hat{\theta}}_{\mathrm{A}j}^{(i)}\right) \\ &\qquad i = 1, 2,\ j = 1, \ldots, 4 \\ u_{\mathrm{L}k}^{(i)} &= -K_{\mathrm{PL}k}^{(i)}\left(\theta_{\mathrm{L}k}^{(i)} - \hat{\theta}_{\mathrm{L}k}^{(i)}\right) - K_{\mathrm{DL}k}^{(i)}\left(\dot{\theta}_{\mathrm{L}k}^{(i)} - \dot{\hat{\theta}}_{\mathrm{L}k}^{(i)}\right) \\ &\qquad i = 1, 2,\ k = 1, \ldots, 6 \end{aligned} \tag{17}$$

where $u_{\mathrm{A}j}^{(i)}$ and $u_{\mathrm{L}k}^{(i)}$ are the actuator torques at Joint j of Arm i and Joint k of Leg i $(i = 1, 2, j = 1, \ldots, 4, k = 1, \ldots, 6)$, and $K_{\mathrm{PA}j}^{(i)}$, $K_{\mathrm{DA}j}^{(i)}$, $K_{\mathrm{PL}k}^{(i)}$, and $K_{\mathrm{DL}k}^{(i)}$ are feedback gains $(i = 1, 2, j = 1, \ldots, 4, k = 1, \ldots, 6)$. In numerical simulations, the bandwidth of the joints is given as 6 Hz for these feedback gains.

3.4. Posture Control

Although all the joints are controlled directly by motors, the robot has no actuator between the feet and the ground. Therefore, it is difficult to control the robot's posture and motion. To stabilize them, the walking motions are modified using feedback signals from touch sensors, since the sensory signals depend on the posture and motion. Specifically, the feedback signals reset the phases of the oscillators and then modify the nominal joint trajectories.

Here, the phase dynamics of Leg Oscillators, which is defined in Eq. (8), is modified by

$$\dot{\phi}_{\mathrm{L}}^{(i)} = \hat{\omega} + g_{1\mathrm{L}}^{(i)} + g_{2\mathrm{L}}^{(i)} \quad i = 1, 2 \tag{18}$$

where $g_{2\mathrm{L}}^{(i)}$ is the term arising due to the feedback signals from the touch sensors of Leg i $(i = 1, 2)$. Function $g_{2\mathrm{L}}^{(i)}$ is designed in the following way: Suppose that $\phi_{\mathrm{land}}^{(i)}$ is the value of phase $\phi_{\mathrm{L}}^{(i)}$ of Leg i Oscillator at the instant when the foot of Leg i lands on the ground $(i = 1, 2)$, and that $\hat{\eta}_{\mathrm{land}}^{(i)}$ is the position of the foot, specifically Joint 5, of Leg i in coordinate axes $\{\boldsymbol{a}_{\mathrm{T}}\}$ fixed in the trunk at that instant, that is, $\hat{\eta}_{\mathrm{land}}^{(i)} = \hat{\eta}_{\mathrm{Sw}}^{(i)}(\phi_{\mathrm{land}}^{(i)})$ $(i = 1, 2)$. When the foot of Leg i touches the ground, the following procedure occurs:

1. Set phase $\phi_{\mathrm{L}}^{(i)}$ of Leg i Oscillator from $\phi_{\mathrm{land}}^{(i)}$ to $\hat{\phi}_{\mathrm{AEP}}$.
2. Switch nominal foot trajectory $\hat{\eta}_{\mathrm{L}}^{(i)}$ of Leg i from nominal foot trajectory $\hat{\eta}_{\mathrm{Sw}}^{(i)}$ for the swing phase to nominal foot trajectory $\hat{\eta}_{\mathrm{St}}^{(i)}$ for the stance phase.
3. Replace parameter $\hat{\eta}_{\mathrm{AEP}}^{(i)}$ in nominal trajectory $\hat{\eta}_{\mathrm{St}}^{(i)}$ with $\hat{\eta}_{\mathrm{land}}^{(i)}$.

Then, function $g_{2\mathrm{L}}^{(i)}$ $(i = 1, 2)$ is given by

$$g_{2\mathrm{L}}^{(i)} = \left(\hat{\phi}_{\mathrm{AEP}} - \phi_{\mathrm{land}}^{(i)}\right)\delta\left(t - t_{\mathrm{land}}^{(i)}\right) \quad i = 1, 2 \tag{19}$$

where $t_{\mathrm{land}}^{(i)}$ is the time when the foot of Leg i lands on the ground $(i = 1, 2)$ and $\delta(\cdot)$ denotes Dirac's delta function. Namely, function $g_{2\mathrm{L}}^{(i)}$ works as a reset of phase $\phi_{\mathrm{L}}^{(i)}$ of Leg i from value $\phi_{\mathrm{land}}^{(i)}$ to nominal value $\hat{\phi}_{\mathrm{AEP}}$ only at the instant that the foot of Leg i lands. As a result, nominal foot trajectory $\hat{\eta}_{\mathrm{L}}^{(i)}$ of Leg i is modified as shown in Fig. 6; in the swing phase, the foot of Leg i continues to follow closed curve $\hat{\eta}_{\mathrm{Sw}}^{(i)}$ in Fig. 5 unless the foot of Leg i touches the ground at point $\hat{\eta}_{\mathrm{land}}^{(i)}$ in axes $\{\boldsymbol{a}_{\mathrm{T}}\}$. Then, the nominal foot trajectory of Leg i changes from nominal foot trajectory $\hat{\eta}_{\mathrm{Sw}}^{(i)}$ for the swing phase to the nominal foot trajectory for the modified stance phase.

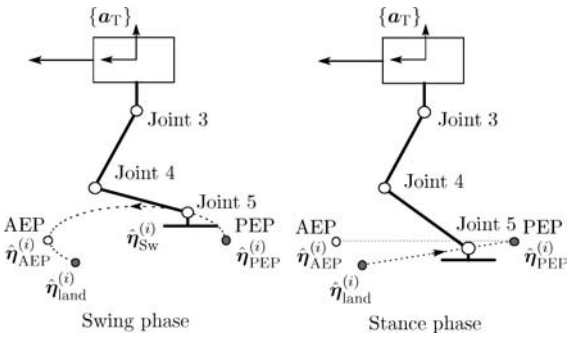

Figure 6. Modified nominal foot trajectory with respect to the touch sensor signal. The nominal foot trajectory changes from the swing phase to the stance phase when the leg touches the ground. The trajectory is modified depending on the timing of the foot's landing. In the swing phase, the nominal foot trajectory follows the closed curve unless the leg touches the ground. When the foot of Leg i lands on the ground at $\hat{\eta}^{(i)}_{\text{land}}$, the nominal foot trajectory for the stance phase is modified by replacing parameter $\hat{\eta}^{(i)}_{\text{AEP}}$ in nominal trajectory $\hat{\eta}^{(i)}_{\text{St}}$ with $\hat{\eta}^{(i)}_{\text{land}}$ $(i = 1, 2)$. Then, the trajectory changes to the modified stance phase.

4. Numerical Simulations

In this section, we verify the effectiveness of the proposed locomotion control system by numerical simulations. In particular, the numerical simulations determine whether the proposed control system responds effectively to environmental changes and disturbances. To verify the effectiveness, we carry out simulations not only with the proposed locomotion control system (Proposed), but also simulations without the touch sensor signal (Without T.S.S.) and compare the results. Note that in the case without the touch sensor signal, the nominal trajectories for all the joints are not modified with respect to the foot's landing on the ground; that is, in that sense all the trajectories are completely open-loop ones. At the beginning, the robots both with the proposed locomotion control system and without the touch sensor walk stably in a fixed environmental situation. We then gradually alter some environmental conditions or cause disturbances to the robots as they walk, and investigate whether the robots can continue to walk adaptively to the changes and disturbances. Table 1 shows the physical parameters of the biped robot HOAP-1 ((Fujitsu Automation Ltd.,), see Fig. 7), used in the numerical simulations.

4.1. Parameter Design

As explained in Section 3.2, the control system has parameters $\hat{A}$, $\hat{B}$, $\hat{C}$, $\hat{\psi}$, $\hat{\delta}$, K_{T}, K_{A}, K_{L}, $\hat{T}_{\text{Sw}}$, $\hat{\beta}$, and $\hat{S}$.

Table 1. Physical parameters of HOAP-1.

Link	Weight [kg]	Length [m]
Trunk	2.34	0.20
Leg	1.32	0.28
Arm	0.43	0.22
Total	5.84	0.48

Figure 7. HOAP-1 (Fujitsu Automation Ltd.).

These parameters are set to be constant depending on a fixed environmental situation. Nominal swing phase duration $\hat{T}_{\text{Sw}}$ is set at 0.3 s, and nominal duty ratio $\hat{\beta}$ and nominal stride $\hat{S}$ are determined according to nominal locomotion speed $\hat{v}$ (16) in a fixed environmental situation. The following parameters are set geometrically: $\hat{A} = 10^\circ$, $\hat{\psi} = -150^\circ$, and $\hat{\delta} = 2^\circ$. Large values are used for gain constants to keep the nominal gait pattern during walking as follows: $K_{\text{T}} = 5$, $K_{\text{A}} = 5$, and $K_{\text{L}} = 10$. As described above, the posture and motion of the robot are crucial for controlling the robot's walking. In particular, since the roll and the pitch motions of the robot heavily influence walking, parameters $\hat{B}$ and $\hat{C}$ are determined so that the robot walks stably. Stability in walking is examined using a Poincaré map (see Appendix C).

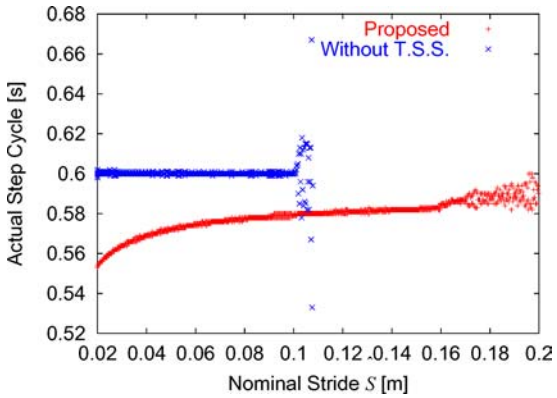

Figure 8. Actual step cycle versus nominal stride $\hat{S}$. In this numerical simulation, as a variation of the environment, the locomotion speed of the robot changes by varying nominal stride $\hat{S}$ gradually. In the case with the proposed locomotion control system (Proposed) the robot walks in almost all this range of locomotion speed while in the case without the touch sensor signal (Without T.S.S.) the robot falls over soon around $\hat{S} = 10$ cm.

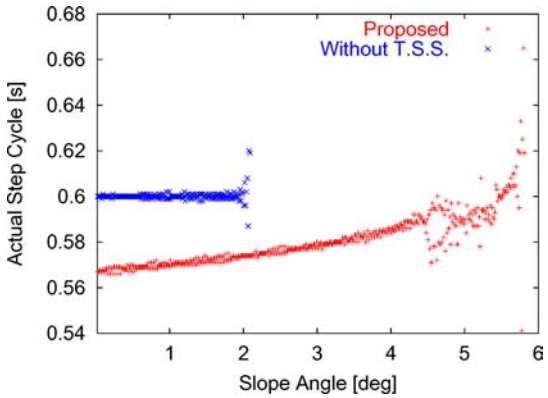

Figure 9. Actual step cycle versus the floor's slope angle. In this numerical simulation, the floor's slope angle varies gradually as an environmental change. The robot with the proposed locomotion control system (Proposed) walks in almost all this range of floor slope angles. On the other hand, the robot without the touch sensor signal (Without T.S.S.) falls over soon at a slope angle of around 2°.

4.2. *Change of Locomotion Speed*

In this numerical simulation, the robot's locomotion speed changes gradually as an environmental change. In particular, the robot's stride changes in order to vary the locomotion speed. The parameters are given as follows: $\hat{S} = 2$ cm, $\hat{\beta} = 0.5$, $\hat{B} = 1°$, and $\hat{C} = 13°$. The nominal locomotion speed changes by varying nominal stride $\hat{S}$ from 2 cm to 20 cm according to Eq. (16). That is, nominal locomotion speed $\hat{v}$ changes from 6.7 cm/s to 67 cm/s. Figure 8 shows the profiles of the actual step cycle with respect to nominal stride $\hat{S}$, where the actual step cycle indicates the time interval from one left-foot landing on the ground to the next left-foot landing. This figure reveals that in the case with the proposed locomotion control system the robot continues to walk in almost all this range of locomotion speed, whereas in the case without the feedback signal from the touch sensors, the robot falls over soon around $\hat{S} = 10$ cm. It also reveals that the robot with the proposed locomotion control system achieves robust walking by changing the actual step cycle adaptively according to the change of locomotion speed.

4.3. *Change of Floor's Slope Angle*

Here, as an example of a change of environment, the floor's slope angle changes gradually. The parameters are given as follows: $\hat{S} = 5$ cm, $\hat{\beta} = 0.5$, $\hat{B} = 2°$, and $\hat{C} = 13°$. The slope angle of the floor changes from 0° to 6°. Figure 9 shows the profiles of the actual step cycle versus the floor's slope angles, and the figure implies that the robot with the proposed locomotion control system continues to walk in almost all this range of floor slope angles. On the other hand, the robot without the feedback signals from the touch sensors falls over soon at a slope angle of around 2°. The figure also implies that in the case with the proposed locomotion control system, the robot obtains robust walking by changing the actual step cycle adaptively depending on the slope angle.

4.4. *Recovery from Disturbance*

Since the robot's walking in a fixed environment is locally stable according to the stability criterion determined with a Poincaré map, the walking motion can recover from small disturbances. In this numerical simulation, we disturb the robot a lot without changing the environmental situation, then investigate whether the robot recovers. Since the posture and motion of the robot, particularly the roll and the pitch motions, are crucial in walking as described above, the roll motion or the pitch motion is disturbed when the robot walks stably and the robot is supported by only one leg. Specifically, when the robot is supported by the right leg (Leg 2) and the swing leg is at the top of the swing-leg trajectory, that is, $\phi_{\mathrm{L}}^{(1)} = \hat{\phi}_{\mathrm{AEP}}/2$, angular velocity $\dot{\theta}_{\mathrm{T1}}$ of the roll angle or angular velocity

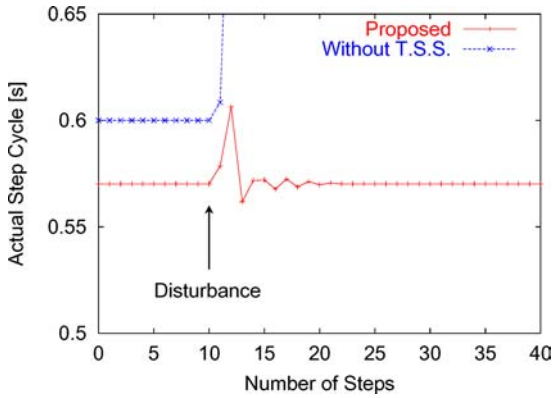

Figure 10. Actual step cycle versus number of steps when the robot is disturbed. In this numerical simulation, when the robot is supported by only the right leg, angular velocity $\dot{\theta}_{T2}$ of the pitch angle of the trunk changes discontinuously by adding -4.0 rad/s. In the case with the proposed locomotion control system (Proposed), a few steps after being disturbed the actual step cycle converges to that of stable walking and the robot recovers. In the case without touch sensor signals (Without T.S.S.), however, the actual step cycle diverges and the robot falls over soon after being disturbed.

$\dot{\theta}_{T2}$ of the pitch angle of the trunk changes discontinuously by adding Δ_{T1} or Δ_{T2}, respectively. Through a simulation we investigate whether the robot recovers to stable walking with respect to Δ_{T1} and Δ_{T2}. It is considered that the robot recovers if the robot continues to walk without falling over for more than 20 steps after being disturbed. The parameters are given here as follows: $\hat{S} = 4$ cm, $\hat{\beta} = 0.5$, $\hat{B} = 2^\circ$, and $\hat{C} = 6^\circ$. The simulation examines disturbances Δ_{T1} and Δ_{T2} in increments of ± 0.1 rad/s from 0 rad/s. The numerical simulation reveals that in the case with the proposed locomotion control system the robot recovers from -3.1 rad/s to 5.7 rad/s with respect to Δ_{T1} and from -4.2 rad/s to 4.2 rad/s with respect to Δ_{T2}. On the contrary, in the case without feedback signals from the touch sensors, the robot achieves the recovery from -2.1 rad/s to 4.6 rad/s with respect to Δ_{T1} and from -3.5 rad/s to 3.8 rad/s with respect to Δ_{T2}. Figure 10 shows the actual step cycle versus the step number using $\Delta_{T2} = -4.0$ rad/s. This figure implies that in the case with the proposed locomotion control system, a few steps after being disturbed the actual step cycle converges to that of stable walking, and the robot recovers to stable walking. In the case without touch sensor signals, however, the actual step cycle diverges and the robot falls over soon after being disturbed.

The numerical results reveal that the robot with the proposed locomotion control system can walk adaptively to these environmental variations and disturbances by changing the step cycle. On the other hand, the robot without the touch sensor signal cannot change the step cycle adaptively since the nominal trajectories of the joints are open-loop and cannot achieve robust walking. In the case with the proposed locomotion control system, the adaptive change of the step cycle due to the sensory feedback from the touch sensor chiefly comes from the following: When the foot of Leg i lands on the ground, phase $\phi_L^{(i)}$ of Leg i Oscillator is reset to nominal value $\hat{\phi}_{AEP}$. Therefore, in the step cycle, the actual swing phase duration depends on the timing of the foot's landing on the ground. As a result, the actual step cycle changes as shown in Fig. 11.

It should be noted that our proposed locomotion control system using nonlinear oscillators has a crucial discrepancy between a biped robot and a quadruped robot. In the control system, phase reset of the oscillators results in changes of the phase differences between the oscillators and the step cycle, as described above. Our previous study (Tsujita et al., 2001) showed that a quadruped robot with a proposed control system composed of nonlinear oscillators walks adaptively by

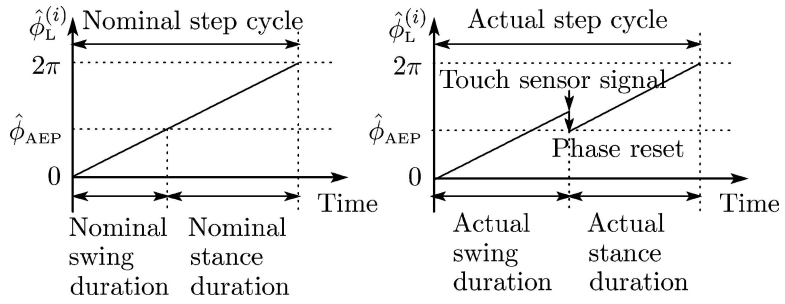

Figure 11. Schematics of nominal and actual phase $\phi_L^{(i)}$ of Leg i Oscillator with respect to time. The phase is reset to nominal value $\hat{\phi}_{AEP}$ depending on the timing of touch sensor signals. As a result, the actual step cycle changes due to the phase reset.

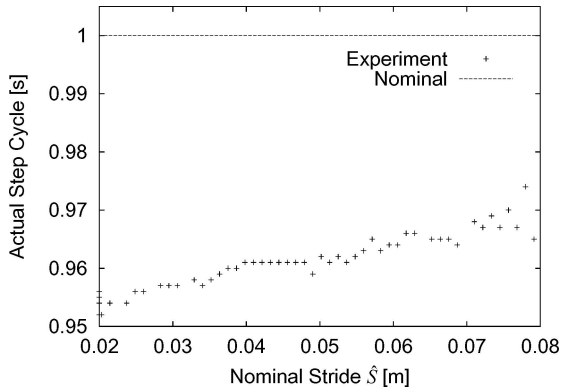

Figure 12. Actual step cycle versus nominal stride $\hat{S}$. In this hardware experiment, the locomotion speed varies by changing nominal stride $\hat{S}$ gradually as a environmental variation. The robot with the proposed locomotion control system walks in this range of locomotion speed by changing the step cycle adaptively.

changing the phase differences, and as a result, varying the gait patterns. For example, when the locomotion speed increases the gait pattern changes from a walk to a trot, and when the floor changes from flat to an upslope, the gait pattern shifts to a bounce by changing the phase differences. This implies that in the quadruped robot the phase difference has a lot of influence on the walking motion and works as an internal state to achieve robust walking, moving freely during walking. On the contrary, the gait pattern of the biped robot cannot change so much from the nominal gait pattern by varying the phase differences, since the change of the gait pattern easily decreases the stability of walking. That is, the biped robot uses high gain constants in Eq. (9) not to fluctuate the gait pattern. Therefore, the biped robot does not have such an internal state to move freely during walking and achieve robust walking. Instead, the biped robot primarily uses the adaptive change of the step cycle intermittently depending on variations of the environments and disturbances.

5. Hardware Experiments

In this section, we carry out hardware experiments using the biped robot, HOAP-1 ((Fujitsu Automation Ltd.,), see Fig. 7) to verify that the robot with the proposed locomotion control system can walk adaptively to environmental changes. In the experiments, a host computer (Equivalent Pentium III 700 MHz, RT-Linux) is used to compute the nominal joint trajectories and solve the phase dynamics of the oscillators. The robot has a power supply cable and a Universal Serial Bus (USB) cable. The robot receives the nominal trajectories as command signals via the USB cable from the host computer every 1 ms.

Similarly to the numerical simulations, in a fixed environmental situation we determine the parameters in the controller so that the robot can walk stably. Then, we investigate only a few environmental changes

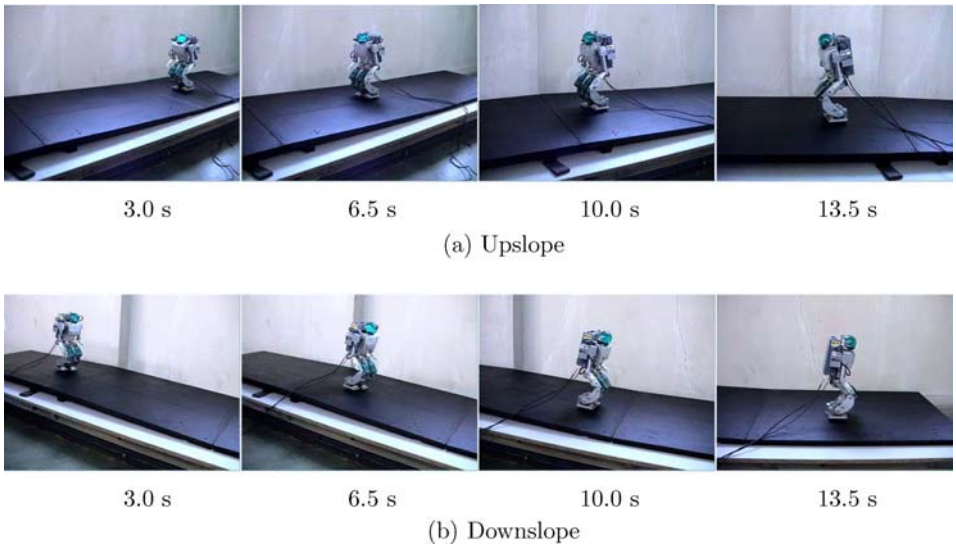

Figure 13. Slopes in hardware experiments. (a) and (b) show upslope and downslope, respectively. At the beginning, the biped robot walks on the flat surface, then on the slope, and finally again on the flat surface. The angle of both slopes is about 2.35°.

to ascertain whether the robot can continue to walk adaptively by using the proposed locomotion control system.

5.1. *Change of Locomotion Speed*

In this hardware experiment, as a change of the environment, the locomotion speed of the robot changes gradually. Specifically, changing the robot's stride alters the locomotion speed. The parameters are given as follows: $\hat{S} = 2\,\text{cm}$, $\hat{\beta} = 0.7$, $\hat{B} = 7^\circ$, and $\hat{C} = 13^\circ$. The nominal locomotion speed varies by changing nominal stride $\hat{S}$ from 2 cm to 8 cm according to Eq. (16); that is, nominal locomotion speed $\hat{v}$ changes from 2.9 cm/s to 11.4 cm/s. Figure 12 shows the profiles of the actual step cycle with respect to nominal stride $\hat{S}$. This figure reveals that the robot with the proposed locomotion control system walks adaptively to the change of the locomotion speed by changing the step cycle.

5.2. *Change of Floor's Slope Angle*

Here, the floor's slope angle changes discontinuously as an environmental variation. Specifically, at the beginning the robot walks on a level surface, then on the slope, and finally again on the flat surface (see Fig. 13). Two types of slope, upslope and downslope, are examined. The angle of both slopes is about 2.35°. The parameters are given as follows: $\hat{S} = 3$ cm, $\hat{\beta} = 0.7$, $\hat{B} = 7^\circ$, and $\hat{C} = 13^\circ$ (for upslope), 8° (for downslope). Figures 14(a) and (b) show the profiles of the actual step cycle versus the step number. These figures imply that the robot with the proposed locomotion control system walks adaptively and changes the step cycle depending on the discontinuous change of the floor's slope angle.

These experimental results verify that the robot with the proposed locomotion control system can walk adaptively to these environmental variations by changing the step cycle.

6. Discussion

In the field of neuroethology, many studies have been conducted to elucidate the control system in walking of animals, revealing that walking motions are generated by a central pattern generator (CPG) (Grillner, 1981; Orlovsky et al., 1999). The CPG comprises sets of neural oscillators and generates rhythmic signals that activate animals' limbs. In the CPG, the amplitudes and the phases of the rhythmic signals are modified in response to sensory feedback signals that come from peripheral nerves. As a result, the motions of the limbs are also modified adaptively and robust motions are achieved against environmental variations. The CPG has been widely modeled using nonlinear oscillators and many studies has been conducted using CPG models based on quadruped robots (Lewis and Bekey, 2002; Fukuoka et al., 2003), biped robots (Lewis et al., 2003; Nakanishi et al., 2004), multi-legged robots (Akimoto et al., 1999; Inagaki et al., 2003), a simulated salamander (Ijspeert, 2001), and human models (Taga et al., 1991; Taga, 1995; Ogihara and Yamazaki, 2001; Yamasaki et al., 2003).

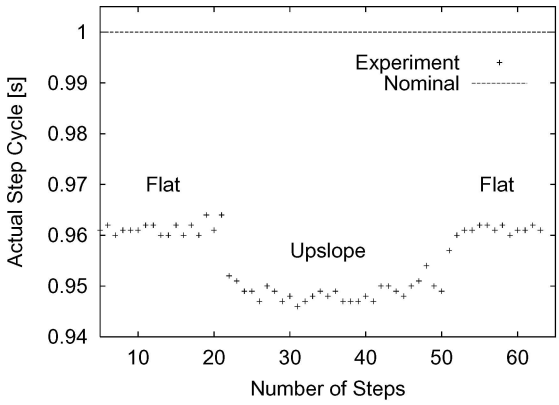

(a) Upslope

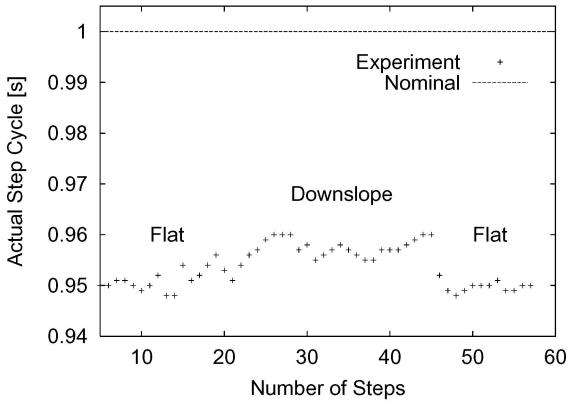

(b) Downslope

Figure 14. Actual step cycle versus number of steps. In these hardware experiments, the floor's slope angle changes discontinuously as shown in Fig. 13. The slopes are upsploe in (a) and downslope in (b). The robot with the proposed locomotion control system walks adaptively by changing the step cycle depending on the environmental situations.

In this paper, we proposed a locomotion control system for a biped robot using nonlinear oscillators. The robot was driven by rhythmic signals from the oscillators, since the nominal trajectories of the joints were designed by the functions of the oscillators' phases. The essential point in the control system is that the phases of the oscillators are reset and the nominal trajectories are modified depending on feedback signals from touch sensors. Numerical simulations and hardware experiments revealed that three-dimensional robust walking was achieved by changing the step cycle adaptively to environmental variations. A recent study investigated the role for the phase reset in human walking (Yamasaki et al., 2003), whereas this paper suggested adaptability in the control of bipedal locomotion from the engineering point of view.

Appendix A: Reaction Force from the Ground

Contact between the foot and the ground is modeled as the contact between the touch sensors on the foot and the ground. When the touch sensor is in contact with the ground, the sensor is constrained on the ground and receives a reaction force from the ground. In numerical simulations, to avoid the complexity of the impact model between the foot and the ground, reaction force $\lambda_j^{(i)\mathrm{T}} = [\,\lambda_{j1}^{(i)}\ \lambda_{j2}^{(i)}\ \lambda_{j3}^{(i)}\,]$ of Sensor j of Leg i from the ground expressed in axes $\{\boldsymbol{a}_0\}$ ($i = 1, 2$, $j = 1, \cdots, 4$) is modeled as a spring with a damper (Adolfsson et al., 2001), and is given by

$$\lambda_j^{(i)} = \begin{cases} -K_{\mathrm{S}}\left(r_{\mathrm{S}j}^{(i)} - \bar{r}_{\mathrm{S}j}^{(i)}\right) - D_{\mathrm{S}}\dot{r}_{\mathrm{S}j}^{(i)} & r_{\mathrm{S}j3}^{(i)} \le 0 \\ 0 & r_{\mathrm{S}j3}^{(i)} > 0 \end{cases} \qquad i = 1, 2,\ j = 1, \ldots, 4 \tag{20}$$

where $K_{\mathrm{S}} = \mathrm{diag}(K_{\mathrm{S1}}, K_{\mathrm{S2}}, K_{\mathrm{S3}})$, $D_{\mathrm{S}} = \mathrm{diag}(D_{\mathrm{S1}}, D_{\mathrm{S2}}, D_{\mathrm{S3}})$, and $r_{\mathrm{S}j}^{(i)}$ and $\bar{r}_{\mathrm{S}j}^{(i)}$ are the position vector of Sensor j of Leg i and the position vector on which Sensor j of Leg i is constrained, respectively, expressed in axes $\{\boldsymbol{a}_0\}$ ($i = 1, 2$, $j = 1, \ldots, 4$). Specifically, the parameters are set to $K_{\mathrm{S1}} = K_{\mathrm{S2}} = K_{\mathrm{S3}} = 2.6 \times 10^4$ N/m and $D_{\mathrm{S1}} = D_{\mathrm{S2}} = D_{\mathrm{S3}} = 2.2 \times 10^2$ Ns/m.

Appendix B: Nominal Foot Trajectory

The nominal foot trajectory is designed here. Note that the nominal trajectory is specifically that of Joint 5 of the leg. The nominal foot trajectory consists of two types of trajectory (see Fig. 5): One is the trajectory for the swing phase and is composed of a closed curve. The other is the trajectory for the stance phase, consisting of a straight line. These trajectories are expressed by the phases of Leg Oscillators in the pitch plane of coordinate axes $\{\boldsymbol{a}_{\mathrm{T}}\}$ fixed in the trunk.

First, the nominal foot trajectory for the swing phase is simply designed using a cycloid trajectory, since the cycloid trajectory has the property that the trajectory speed vanishes at the end of the trajectory and the nominal foot trajectory can touch the ground smoothly. Then, nominal foot trajectory $\hat{\eta}_{\mathrm{Sw}}^{(i)}(\phi_{\mathrm{L}}^{(i)})$ of Leg i for the swing phase ($i = 1, 2$) is given by

$$\hat{\eta}_{\mathrm{Sw}1}^{(i)}(\phi_{\mathrm{L}}^{(i)}) = \begin{cases} \hat{S}\left[\dfrac{\phi_{\mathrm{L}}^{(i)}}{\hat{\phi}_{\mathrm{AEP}}} - \dfrac{1}{2\pi}\sin\left(2\pi\dfrac{\phi_{\mathrm{L}}^{(i)}}{\hat{\phi}_{\mathrm{AEP}}}\right) - \dfrac{1}{2}\right] & 0 \le \phi_{\mathrm{L}}^{(i)} < \hat{\phi}_{\mathrm{AEP}} \\ \hat{S}\left[\dfrac{1}{2} - \dfrac{\phi_{\mathrm{L}}^{(i)} - \hat{\phi}_{\mathrm{AEP}}}{2\pi - \hat{\phi}_{\mathrm{AEP}}} - \dfrac{1}{2\pi}\sin\left(2\pi\dfrac{\phi_{\mathrm{L}}^{(i)} - \hat{\phi}_{\mathrm{AEP}}}{2\pi - \hat{\phi}_{\mathrm{AEP}}}\right)\right] & \hat{\phi}_{\mathrm{AEP}} \le \phi_{\mathrm{L}}^{(i)} < 2\pi \end{cases}$$

$$\hat{\eta}_{\mathrm{Sw}3}^{(i)}(\phi_{\mathrm{L}}^{(i)}) = \begin{cases} \alpha_{\mathrm{up}}\dfrac{\hat{S}}{2\pi}\left[1 - \cos\left(2\pi\dfrac{\phi_{\mathrm{L}}^{(i)}}{\hat{\phi}_{\mathrm{AEP}}}\right)\right] - h_{\mathrm{T}} & 0 \le \phi_{\mathrm{L}}^{(i)} < \hat{\phi}_{\mathrm{AEP}} \\ \alpha_{\mathrm{low}}\dfrac{\hat{S}}{2\pi}\left[1 - \cos\left(2\pi\dfrac{\phi_{\mathrm{L}}^{(i)} - \hat{\phi}_{\mathrm{AEP}}}{2\pi - \hat{\phi}_{\mathrm{AEP}}}\right)\right] - h_{\mathrm{T}} & \hat{\phi}_{\mathrm{AEP}} \le \phi_{\mathrm{L}}^{(i)} < 2\pi \end{cases} \qquad i = 1, 2 \tag{B.1}$$

where α_{up} and α_{low} are ratios to raise the foot with respect to nominal stride $\hat{S}$, and h_{T} is the height from the line that includes points AEP and PEP to the origin of coordinate axes $\{\boldsymbol{a}_{\mathrm{T}}\}$. In this paper, the parameters are set as follows: $\alpha_{\mathrm{up}} = 1.6$, $\alpha_{\mathrm{low}} = 0.2$, and height h_{T} consists of the heights from the line that involves points AEP and PEP to Joint 3 of the leg that is set at 16.5 cm, and from Joint 3 of the leg to the origin of axes $\{\boldsymbol{a}_{\mathrm{T}}\}$. Note that in the case without the touch sensor signal, the nominal foot trajectory for the swing phase is used only for $0 \le \phi_{\mathrm{L}}^{(i)} < \hat{\phi}_{\mathrm{AEP}}$, that is, only the upper part of the closed curve is used (see Section 3.4).

Second, nominal foot trajectory $\hat{\eta}_{\mathrm{St}}^{(i)}(\phi_{\mathrm{L}}^{(i)})$ of Leg i for the stance phase ($i = 1, 2$) is designed as the straight

line that includes points AEP and PEP.

$$\hat{\eta}^{(i)}_{\mathrm{Sp1}}\left(\phi^{(i)}_{\mathrm{L}}\right) = \hat{S}\left(\frac{1}{2} - \frac{\phi^{(i)}_{\mathrm{L}} - \hat{\phi}_{\mathrm{AEP}}}{2\pi - \hat{\phi}_{\mathrm{AEP}}}\right)\hat{\phi}_{\mathrm{AEP}} \le \phi^{(i)}_{\mathrm{L}} < 2\pi$$

$$\hat{\eta}^{(i)}_{\mathrm{Sp3}}\left(\phi^{(i)}_{\mathrm{L}}\right) = -h_{\mathrm{T}}$$

$$i = 1, 2 \quad \text{(B.2)}$$

Appendix C: Stability in Walking

Stability of a periodic motion can be analyzed using a Poincaré map. Steady walking by the robot implies that the walking motion is periodic. Therefore, stability of the walking motion is investigated using a Poincaré map.

First, state variable $x \in \mathbb{R}^4$ is introduced as

$$x^{\mathrm{T}} = [\theta_{\mathrm{T1}}\ \dot{\theta}_{\mathrm{T1}}\ \theta_{\mathrm{T2}}\ \dot{\theta}_{\mathrm{T2}}] \quad \text{(C.1)}$$

where θ_{T1} and θ_{T2} are the roll and the pitch angles of the trunk. In particular, the state when the foot of Leg 1 touches the ground is used as the state on the Poincaré section. The Poincaré map, which is the return map from one point on the Poincaré section to the next point on the Poincaré section, is denoted as $x \mapsto p(x)$, thus

$$x_{i+1} = p(x_i) \quad \text{(C.2)}$$

where x_i is state variable x on the ith intersection with the Poincaré section. Note that fixed point x^* on the Poincaré section satisfies

$$x^* = p(x^*) \quad \text{(C.3)}$$

By adding perturbation $\tilde{x}_i$ from fixed point x^* on the ith intersection with the Poincaré section and linearizing Poincaré map p at fixed point x^*, Jacobian matrix $J(x^*) \in \mathbb{R}^{4\times4}$ of the Poincaré map satisfies

$$\tilde{x}_{i+1} = J(x^*)\tilde{x}_i \quad \text{(C.4)}$$

The stability of the walking motion is ascertained by examining the eigenvalues of Jacobian matrix $J(x^*)$.

Acknowledgment

The authors thank Dr. Katsuyoshi Tsujita for his useful remarks and also thank anonymous reviewers for useful comments. This paper is supported in part by Center of Excellence for Research and Education on Complex Functional Mechanical Systems (COE program of the Ministry of Education, Culture, Sports, Science and Technology, Japan). The authors were funded by grants from the Japan Science and Technology Corporation (JST) under the Core Research for Evolutional Science and Technology Program (CREST).

References

Adolfsson, J., Dankowicz, H., and Nordmark, A. 2001. 3D passive walkers: Finding periodic gaits in the presence of discontinuities. *Nonlinear Dynamics*, 24:205–229.

Akimoto, K., Watanabe, S., and Yano, M. 1999. An insect robot controlled by emergence of gait patterns. *Artificial Life and Robtics*, 3:102–105.

Bessonnet, G., Chessé, S., and Sardain, P. 2004. Optimal gait synthesis of a seven-link planar biped. *The Int. J. of Robotics Research*, 23(10–11):1059–1073.

Chevallereau, C. and Aoustin, Y. 2001. Optimal reference trajectories for walking and running of a biped robot. *Robotica*, 19:557–569.

Fujitsu Automation Limited, http://www.automation.fujitsu.com/en.

Fukuoka, Y., Kimura, H., and Cohen, A.H. 2003. Adaptive dynamic walking of a quadruped robot on irregular terrain based on biological concepts. *The Int. J. of Robotics Research*, 22(3/4):187–202.

Goswami, A. 1999. Postural stability of biped robots and the foot-rotation indicator (FRI) point. *The Int. J. of Robotics Research*, 18(6):523–533.

Grillner, S. 1981. Control of locomotion in bipeds, tetrapods and fish. In *Handbook of Physiology*, American Physiological Society, Bethesda, pp. 1179–1236.

Ijspeert, A.J. 2001. A connectionist central pattern generator for the aquatic and terrestrial gaits of a simulated salamander. *Biol. Cybern.*, 84:331–348.

Inagaki, S., Yuasa, H., and Arai, T. 2003. CPG model for autonomous decentralized multi-legged robot system–generation and transition of oscillation patterns and dynamics of oscillators. *Robotics and Autonomous Systems*, 44:171–179.

Kagami, S., Kitagawa, T., Nishiwaki, K., Sugihara, T., Inaba, M., and Inoue, H. 2002. A fast dynamically equilibrated walking trajectory generation method of humanoid robot. *Autonomous Robots*, 12:71–82.

Kajita, S., Kanehiro, F., Kaneko, K., Fujiwara, K., Yokoi, K., and Hirukawa, H. 2002. A realtime pattern generator for biped walking. In *Proc. Int. Conf. on Robotics and Automation*, pp. 31–37.

Kuramoto, Y. 1984. *Chemical Oscillations, Waves, and Turbulences*, Springer-Verlag: Berlin.

Lewis, M.A. and Bekey, G.A. 2002. Gait adaptation in a quadruped robot. *Autonomous Robots*, 12:301–312.

Lewis, M.A., Etienne-Cummings, R., Hartmann, M.J., Xu, Z.R., and Cohen, A.H. 2003. An in silico central pattern generator: Silicon oscillator, coupling, entrainment, and physical computation. *Biol. Cybern.*, 88:137–151.

Löffler, K., Gienger, M., and Pfeiffer, F. 2003. Sensors and control concept of walking "Johnnie". *The Int. J. of Robotics Research*, 22(3–4):229–239.

Nagasaki, T., Kajita, S., Kaneko, K., Yokoi, K., and Tanie, K. 2004. A running experiment of humanoid biped. In *Proc. Int. Conf. on Intelligent Robots and Systems*, pp. 136–141.

Nakanishi, J., Morimoto, J., Endo, G., Cheng, G., Schaal, S., and Kawato, M. 2004. Learning from demonstration and adaptation of biped locomotion. *Robotics and Autonomous Systems*, 47:79–91.

Ogihara, N. and Yamazaki, N. 2001. Generation of human bipedal locomotion by a bio-mimetic neuro-musculo-skeletal model. *Biol. Cybern.*, 84:1–11.

Ono, K. and Liu, R. 2002. Optimal biped walking locomotion solved by trajectory planning method. *J. of Dynamic Systems, Measurement, and Control*, 124(4):554–565.

Orlovsky, G.N., Deliagina, T., and Grillner, S. 1999. *Neuronal Control of Locomotion: From Mollusc to Man*, Oxford University Press.

Roussel, L., Canudas de Wit, C., and Goswami, A. 1998. Generation of energy-optimal complete gait cycles for biped robots. In *Proc. Int. Conf. on Robotics and Automation*, pp. 2036–2041.

Taga, G., Yamaguchi, Y., and Shimizu, H. 1991. Self-organized control of bipedal locomotion by neural oscillators. *Biol. Cybern.*, 65:147–159.

Taga, G. 1995. A model of the neuro-musculo-skeletal system for human locomotion II. - Real-time adaptability under various constraints. *Biol. Cybern.*, 73:113–121.

Tsujita, K., Tsuchiya, K., and Onat, A. 2001. Adaptive gait pattern control of a quadruped locomotion robot. In *Proc. Int. Conf. on Intelligent Robots and Systems*, pp. 2318–2325.

Vukobratović, M., Borovac, B., Surla, D., and Stokić, D. 1990. *Biped Locomotion-Dynamics, Stability, Control and Application*, Springer-Verlag.

Yamaguchi, J., Soga, E., Inoue, S., and Takanishi, A. 1999. Development of a bipedal humanoid robot - Control method of whole body cooperative dynamic biped walking -. In *Proc. Int. Conf. on Robotics and Automation*, pp. 368–374.

Yamasaki, T., Nomura, T., and Sato, S. 2003. Possible functional roles of phase resetting during walking. *Biol. Cybern.*, 88:468–496.

Shinya Aoi received the B.E. and M.E. degrees from the Department of Aeronautics and Astronautics, Kyoto University, Kyoto, Japan in 2001 and 2003, respectively. He is a Ph.D. candidate in the Department of Aeronautics and Astronautics, Kyoto University. Since 2003, he has been a research fellow of the Japan Society for the Promotion of Science (JSPS). His research interests include dynamics and control of robotic systems, especially legged robots. He is a member of IEEE, SICE, and RSJ.

Kazuo Tsuchiya received the B.S., M.S., and Ph.D. degrees in engineering from Kyoto University, Kyoto, Japan in 1966, 1968, and 1975, respectively. From 1968 to 1990, he was a research member of Central Research Laboratory in Mitsubishi Electric Corporation, Amagasaki, Japan. From 1990 to 1995, he was a professor at the Department of Computer Controlled Machinery, Osaka University, Osaka, Japan. Since 1995, he has been a professor at the Department of Aeronautics and Astronautics, Kyoto University. His fields of research include dynamic analysis, guidance, and control of space vehicles, and nonlinear system theory for distributed autonomous systems. He is currently the principal investigator of "Research and Education on Complex Functional Mechanical Systems" under the 21st Century Center of Excellence Program (COE program of the Ministry of Education, Culture, Sports, Science and Technology, Japan).